

# UPLC-QTOF/MS-based metabolomic analysis of plasma reveals altitude effects on yaks (*Bos grunniens*)

Xiangqiong Meng<sup>1,3</sup> Juan Zhou<sup>2</sup> Jingyi Li<sup>1</sup> Ruidong Wan<sup>2,3</sup> Hongxian Yu<sup>2,3</sup> Qing Wei<sup>1,3\*</sup>

## *Abstract*

The yak is an ideal animal model for the study of adaptation to hypoxia at high altitudes. Its blood metabolites are an important reference index for research regarding adaptation to high-altitude hypoxia and can reflect cellular activity, antioxidant capacity and the metabolic capacity of yaks, thus highlighting the adaptability of the yak to hypoxic environments. The aim of our study was to evaluate differences in the global metabolic profiles of plasma in high- and low-altitude yaks (average age: 3 years old; live weight (LW): 300 ± 50 kg) using untargeted metabolomics. 52 differential metabolites were identified; 13 metabolites such as choline and trimethylamine N-oxide showed upregulated expression and 39 different metabolites such as L-carnitine and oleic acid were downregulated. Most of them were involved in energy, lipid and amino acid metabolism pathways. After analysis, the lysosome, citrate cycle, histidine metabolism and fatty acid biosynthesis changed significantly. The results demonstrate that there were differences in the metabolomes of high- and low-altitude yaks. As altitude increases, the critical pathways involve lysosomes, citrate cycle, histidine metabolism, fatty acid biosynthesis and biosynthesis of unsaturated fatty acids.

---

**Keywords:** yak, different altitudes, plasma, untargeted metabolomics

<sup>1</sup>College of Eco-Environmental Engineering, Qinghai University, Xining, Qinghai, China

<sup>2</sup>Department of Veterinary Medicine, College of Agriculture and Animal Husbandry, Qinghai University, Xining, Qinghai, China

<sup>3</sup>State Key Laboratory of Plateau Ecology and Agriculture, Qinghai University, Xining, Qinghai, China

\*Correspondence: [xwq3519@sina.com](mailto:xwq3519@sina.com) (Q. Wei)

Received February 21, 2021.

Accepted May 11, 2021.

doi: <https://doi.org/10.14456/tjvm.2021.66>

## Introduction

The yak (*Bos grunniens*) is an ancient and primitive species in China. It is a mammal that lives at the highest altitudes of the geographical regions often called the “roof of the world”. Although a rare animal resource, yaks can provide meat, milk and plush wool for breeders (Qiu *et al.* 2012) and they represent an important pillar of animal husbandry in alpine grasslands. The yak is also an extremely rare and valuable gene bank, which integrates the products and performance of all categories of livestock and its genetic resources have always garnered attention and importance (Bao *et al.* 2019; Wang *et al.* 2017). Therefore, the yak has been the focus of research concerning plateau animals.

Most studies involving yaks have focused on the origin of species, breed cultivation, milk production, as well as meat nutritional value and quality. The adaptability of the yak to hypoxia has attracted increased interest and has been studied in terms of morphology (Kalita and Bhattacharya 2003), physiology (Ding *et al.* 2014; Wang *et al.* 2018), genomics (Ma *et al.* 2020; Zhang *et al.* 2016), transcriptomics (Lan *et al.* 2018; Ma 2019), proteomics (Babar *et al.* 2019; Zuo *et al.* 2017), and other aspects. However, few investigations have focused on the role of metabolism in hypoxic adaptation. The metabolism of an organism is the final result of the interaction of various factors, including genetic, physiological and environmental ones. Different altitudes may cause changes in a series of metabolites and metabolites are the end products of cellular regulatory processes. Metabolite levels can be regarded as the ultimate

response of biological systems to genetic or environmental changes (Fiehn 2002).

Metabolomics is an emerging technological and analytical field in systems biology, following genomics, transcriptomics and proteomics (Gertsman and Barshop 2018). The main goal of metabolomics includes the quantitative study of the multiple dynamic responses of organisms to external stimuli, pathophysiological changes and metabolite levels resulting from gene mutations (Nicholson *et al.* 1999). Metabolomics can maximize qualitative and quantitative metabolites in biological systems and reflect the total metabolite information to the greatest extent. Therefore, metabolomics has a lot of information to further explain the physiological condition of an organism using high-throughput methods to study metabolites in biological samples. Untargeted metabolomics is especially useful when there is no a priori metabolic hypothesis. Liquid chromatography coupled to mass spectrometry (LC-MS) has been the preferred choice for untargeted metabolomics, given the versatility in metabolite coverage and the sensitivity of these instruments.

This study aimed to use an ultra-high-performance liquid chromatography-triple/time-of-flight mass spectrometry (UPLC-QTOF/MS) approach to evaluate differences in the global metabolic profiles of plasma in high- and low-altitude yaks and to further explore the effects of different altitudes on the metabolism and normal survival of the yak. The experimental process is shown in Fig 1. The results may provide a reference for the scientific breeding of yaks and may elucidate the mechanisms by which yaks have physiologically adapted to the metabolic cost of maintaining body function while being exposed to different altitudes.

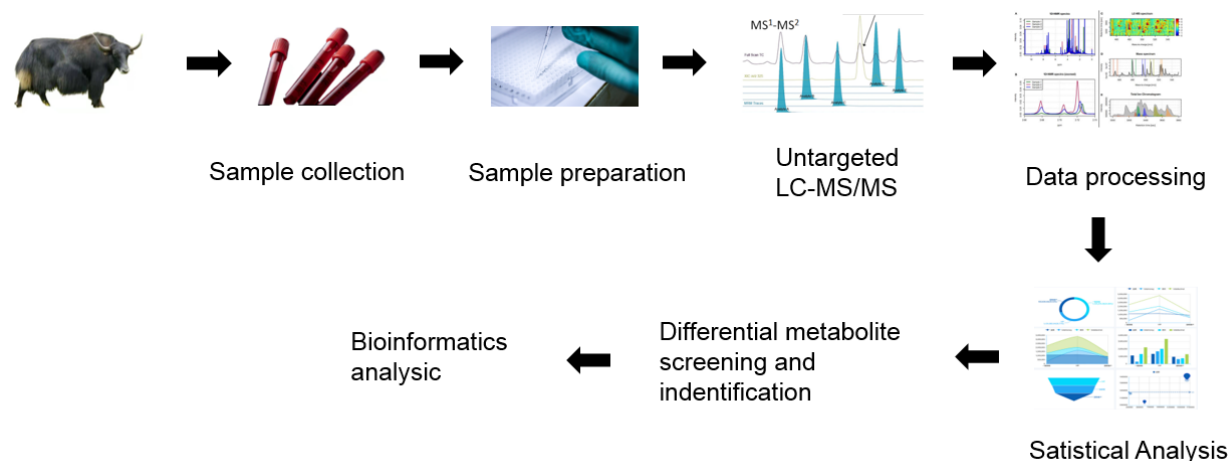


**Figure 1** Experimental flowchart.

## Materials and Methods

**Animals:** In total, we studied 12 yaks (6 females and 6 males) about 3 years old from the pastoral area of Qilian County (altitude 4000 m, 100.25° E, 38.18° N) and Xunhua County (altitude 2600 m, 102.49° E, 35.85° N), Qinghai, China. The live weight (LW) of the yaks was about  $300 \pm 50$  kg. Animals from Qilian County represented a high-altitude group, designated as HA. Yaks from Xunhua County comprised a low-altitude cohort termed as LA. The weights and ages of the yaks

were similar. This study was approved by the Institutional Animal Care and Use Committee of Qinghai University (Xining, China) and all procedures were performed in accordance with the approved guidelines.

**Sample collection:** Approximately 4 mL of blood was collected from the neck of the yaks. After collection, the tubes were centrifuged at  $1699 \times g$  for 10 mins at 4°C to remove blood cells and plasma was immediately stored at -80°C prior to further processing.

**Sample pretreatment:** All samples were thawed at 4°C, and 100-µL aliquots were mixed with 400 µL of cold solution (methanol/acetonitrile = 1:1, v/v) to remove proteins. The mixture was centrifuged at 14,000 × g for 20 mins at 4°C. The supernatant was dried in a vacuum centrifuge. For LC-MS analysis, whole samples were treated with an acetonitrile water solution (acetonitrile/water = 1:1 v/v) for testing.

**UHPLC analysis:** All plasma samples were separated by UHPLC (1290 Infinity LC, Agilent Technologies, USA), equipped with an HILIC column using a 1.7 µm, 2.1 mm × 100 mm ACQUIY UPLC BEH column (Waters, Ireland). In the electrospray ionization (ESI) positive and negative ion modes, the mobile phase contained 25 mM ammonium hydroxide in water, with A = 25 mM ammonium acetate and B = acetonitrile. The elution gradient was 95% B for 0.5 min, which was linearly reduced to 65% over 6.5 mins and then reduced to 40% over 1 min, maintained for 1 min and then returned to 95% in 0.1 min for approximately 3 mins of equilibrium.

Samples were placed in an autosampler at 4°C throughout the analysis. To avoid the influence of instrument detection signal fluctuations, we used a random injection sequence. Regular intervals inserting a Quality control (QC) sample (every 8 samples) throughout the analytical process provided a set of data from which stability and repeatability could be assessed.

**Quadrupole-time-of-flight analysis:** After UHPLC separation, mass spectrometry analysis was performed with a quadrupole time-of-flight platform (AB Sciex Triple TOF 6600) at Shanghai Applied Protein Technology Co., Ltd. The conditions were as follows: ion source gas 1 (Gas 1) as 40, ion source gas 2 (Gas 2) as 80, curtain gas (CUR) as 30, a source temperature of 650°C and ion spray voltage floating (ISVF) of 5000 V (+) and -5000 V (-). Secondary mass spectrometry data was acquired using information-dependent acquisition (IDA) with the high sensitivity mode selected. The parameters were set as follows: collision energy (CE) fixed at 35 V with ± 15 eV, de-clustering potential (DP) at ± 60 V, excluded isotopes within 4 Da; ten candidate ions were monitored per cycle.

**Data analysis:** The original data generated by UPLC-Q-TOF/MS was converted to MzXML files with Proteo Wizard MS Convert, before being imported into the XCMS software and filtered through XCMS analysis. For peak selection, the parameters were set as follows: centWave m/z = 25 ppm, peakwidth = c (10, 60), prefilter = c (10, 100) and bw = 5, mzwid = 0.025, minfrac = 0.5 at peak grouping. More than 50% of the variables with non-zero measurement values in at least one group remained in the extracted ion features. Compound identification of metabolites by MS/MS spectra and structural identification of metabolites were performed by mass matching (< 25 ppm) and secondary spectrogram matching, which should be searched and compared using the laboratory database established with available authentic standards. Thereafter, the processed data was uploaded before

importing into SIMCA-P14.1 (Umetrics, Umea, Sweden) after normalization of total peak intensity, where it was subjected to multivariate data analysis, including Pareto-scaled principal component analysis (PCA), supervised partial least squares-discriminate analysis (PLS-DA) and orthogonal partial least-squares discriminant analysis (OPLS-DA). Response permutation testing and 7-fold cross-validation were used to evaluate the above-mentioned models. Metabolites with variable importance in the projection (VIP) scores > 1 and  $P < 0.05$  were handled with unidimensional statistical analysis using R software, such as the t-test, volcano plot analysis and variation ratio analysis.

For bioinformatics analysis, metabolite relative expression data was used to perform hierarchical clustering analysis. For this purpose, Cluster v.3.0 (<http://bonsai.hgc.jp/~mdehoon/software/cluster/software.htm>) and Java Treeview software (<http://jtreeview.sourceforge.net>) were used. The Euclidean distance algorithm for similarity measures and average linkage clustering algorithm (clustering uses the centroids of the observations) for clustering were selected when performing hierarchical clustering. To further explore the impact of differentially expressed metabolites, enrichment analysis was performed. KEGG pathway enrichment analyses were used based on the Fisher's exact test and pathways with P value under a threshold of 0.05 were considered significant. For metabolite annotation and pathway analysis, we performed BLAST searches of the online Kyoto Encyclopedia of Genes and Genomes (KEGG) database (<http://geneontology.org/>) to retrieve their COs, which were subsequently mapped to pathways in KEGG11 and data on the corresponding KEGG pathways was extracted.

## Results

**Untargeted metabolomics analysis:** A total of 16,756 metabolite ion peaks were extracted from all samples and analyzed by PCA. The distribution of metabolic profiles for the experimental and QC samples in PCA are shown in Fig 2a. QC injections were clustered tightly in the PCA space, indicating that instrument volatility was small and that the experiment was reproducible. Therefore, the experimental data was objective and reliable, the differences in metabolic profiles could describe biological differences and the data could be used for subsequent analysis.

**Inter-group PCA analysis:** UHPLC-Q-TOF/MS metabolomics profiling for HA and LA produced a total of 9,227 ion peaks under positive modes. After Pareto scaling, PCA indicated differences between HA and LA groups. As shown in Fig 2a, we observed clear separation of HA and LA, which indicated that the spectrum of metabolism in the two groups had changed.

**Inter-group PLS-DA and OPLS-DA analysis:** First, we screened marker metabolites from comprehensive metabolomics data and established correct discriminant models using PLS-DA. PLS-DA score plots showed a clear distinction between the two

groups ( $R2Y = 1$ ,  $Q2 = 0.946$ ; Fig 2b). Thereafter, OPLS-DA was corrected on the basis of PLS-DA to filter out noise that was irrelevant to classification information. The OPLS-DA score plot is shown in Fig 2c ( $R2Y = 1$ ,  $Q2 = 0.921$ ). The permutation plot indicated that the original OPLS-DA model was valid and no overfitting was found ( $R2 = 0.9589$ ,  $Q2 = -0.09337$ ; Fig 2d). Through these analytical methods, we established a relationship model between metabolite expression levels and the sample category and realized the prediction of the sample category, thereby assisting the screening of marker metabolites.

**Univariate statistical analysis:** Volcano plot analysis results are shown in Fig 3, illustrating the significance of metabolite changes between the two samples. Red points represent differential metabolites with  $FC > 1.5$  and  $P < 0.05$ , which can help in screening potential marker metabolites.

**Metabolites with significant differences between groups:** A total of 25 differential metabolites (ESI (+)) were identified between the HA and LA groups based on the criteria of  $VIP > 1$  and according to the OPLS-DA model and univariate statistical analysis (Table 1). Among them, twenty-three metabolites were significantly different metabolites ( $VIP > 1$  and  $P < 0.05$ ) and the remaining two were differential metabolites ( $VIP > 1$  and  $0.05 < P < 0.1$ ).

**Bioinformatics analysis:** To display relationships comprehensively and intuitively between samples and expression patterns of metabolites in different samples, we performed hierarchical clustering for each group of

samples. Metabolites gathered in the same cluster showed similar expression patterns. A heatmap of the Spearman rank-order correlation coefficient after hierarchical cluster analysis indicated that metabolite abundances were different in the HA and LA groups (Fig 4). Although some metabolites also showed similarities, significantly different metabolites were identified which could distinguish the two groups.

Significantly different metabolite correlation analysis results are shown in Fig 5a. The metabolites shown in the Figure are all significantly related metabolites ( $P < 0.05$ ), where blue represents a negative correlation and red represents a positive correlation. The size of the circle is the P value and the depth of the color represents the magnitude of the correlation. A positive correlation implies that the expression trends of the two are the same or similar in function and category, while a negative correlation implies the opposite.

**KEGG metabolic pathway analysis of differential metabolites:** We analyzed and calculated the significance level of metabolite enrichment of each pathway using the Fisher's exact test to determine signal transduction pathways and metabolic pathways with significant changes. Fig 5b presents KEGG pathway enrichment analysis results of the differentially expressed metabolites in the HA vs. LA groups. The results show that histidine metabolism, TCA cycle, fatty acid biosynthesis, glycine, serine and threonine metabolism, biosynthesis of unsaturated fatty acids and glyoxylate and dicarboxylate metabolism had undergone significant changes.

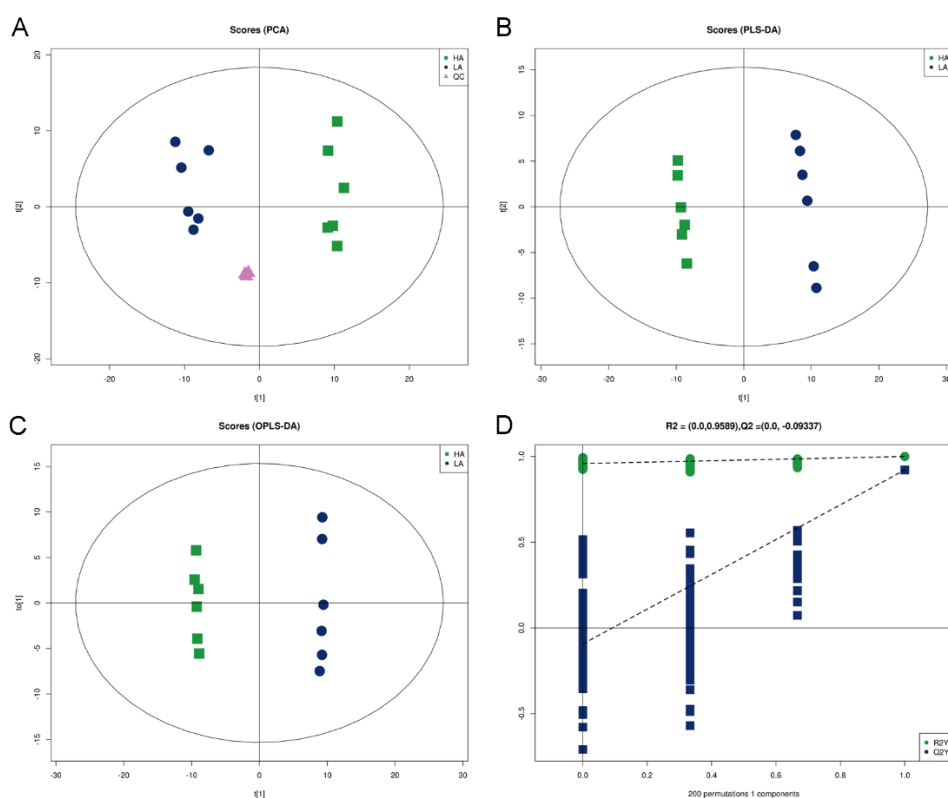


**Figure 2** Metabolomic analysis of all samples from LA and HA groups. The PCA model (a), PLS-DA model (b), and OPLS-DA model (c) showed differences between LA and HA groups, respectively. The permutation plot was used to monitor the stable and reliable OPLS-DA model (d).

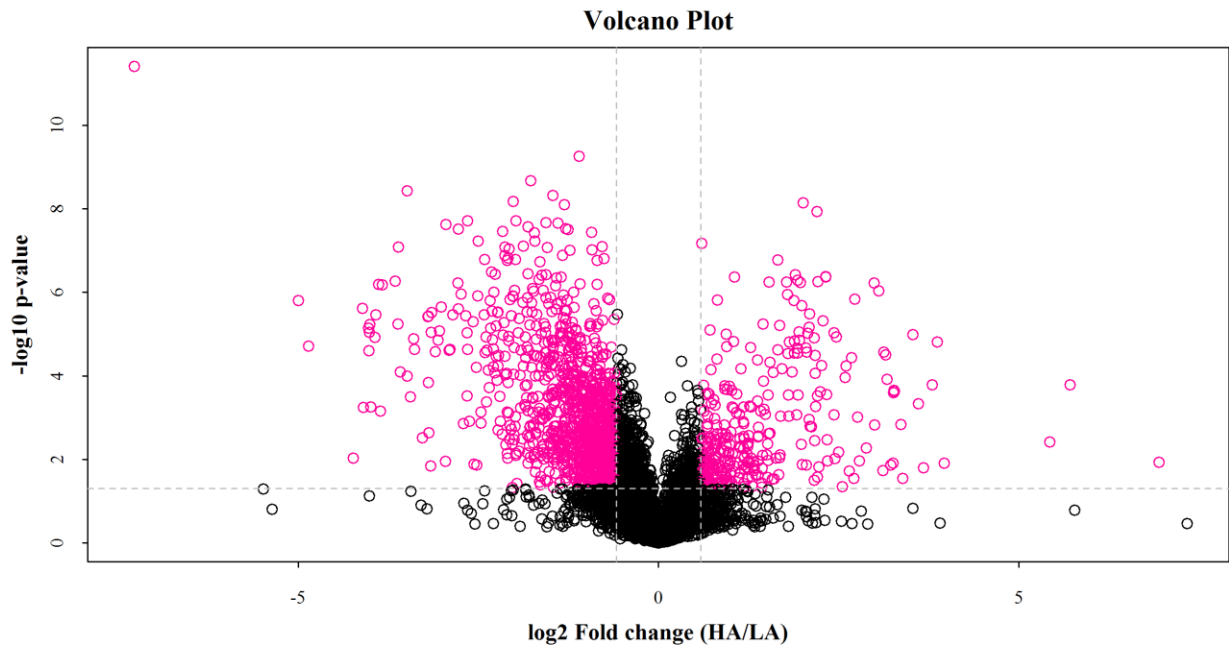


Figure 3 Volcano Plot analysis of differential metabolites.

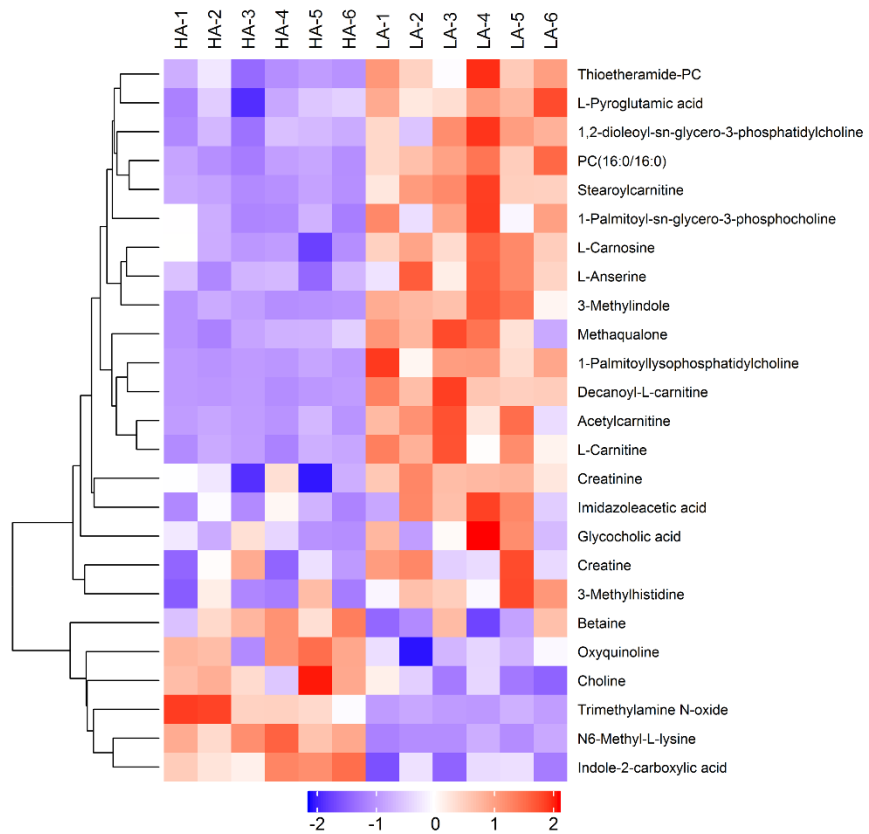
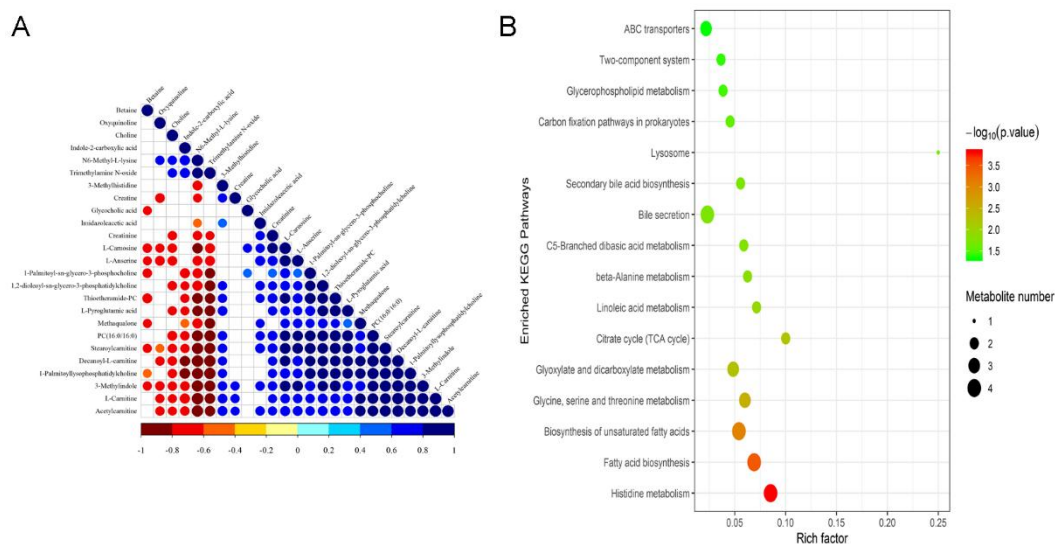


Figure 4 Heatmap of the Spearman rank-order correlation analysis.

**Table 1** Differential metabolites identified between the HA and LA groups

| Ionization mode | Metabolite                                    | VIP    | Fold change | P-value  | m/z     | Rt(s)   | Accession no |
|-----------------|---|--------|-------------|----------|---------|---------|--------------|
| ESI (+)         | L-Carnitine                                   | 20.894 | 0.478       | 0.000108 | 162.112 | 348.051 | M161T526     |
| ESI (+)         | PC(16:0/16:0)                                 | 16.294 | 0.282       | 0.000003 | 756.555 | 146.034 | M162T348_2   |
| ESI (+)         | Acetylcarnitine                               | 12.876 | 0.347       | 0.000327 | 204.123 | 301.477 | M757T146_1   |
| ESI (+)         | Choline                                       | 7.857  | 1.824       | 0.005626 | 104.107 | 265.294 | M204T301     |
| ESI (+)         | 1-Palmitoyl-sn-glycero-3-phosphocholine       | 7.295  | 0.665       | 0.001947 | 496.340 | 193.418 | M104T265_2   |
| ESI (+)         | Trimethylamine N-oxide                        | 6.978  | 12.187      | 0.000461 | 76.075  | 326.337 | M496T193_2   |
| ESI (+)         | Betaine                                       | 6.280  | 1.986       | 0.044115 | 118.086 | 455.203 | M76T326      |
| ESI (+)         | Thioetheramide-PC                             | 6.062  | 0.553       | 0.000292 | 780.553 | 143.479 | M118T455     |
| ESI (+)         | Creatinine                                    | 5.207  | 0.830       | 0.005673 | 114.066 | 167.058 | M781T143_1   |
| ESI (+)         | 3-Methylindole                                | 3.371  | 0.095       | 0.000013 | 132.080 | 36.717  | M114T167_2   |
| ESI (+)         | 1,2-dioleoyl-sn-glycero-3-phosphatidylcholine | 2.869  | 0.595       | 0.000940 | 768.588 | 140.680 | M132T37      |
| ESI (+)         | N6-Methyl-L-lysine                            | 2.309  | 3.459       | 0.000001 | 161.128 | 526.249 | M769T141     |
| ESI (+)         | 1-Palmitoyllysophosphatidylcholine            | 2.263  | 0.209       | 0.000034 | 538.385 | 188.251 | M538T188     |
| ESI (+)         | Oxyquinoline                                  | 2.043  | 1.314       | 0.014874 | 146.059 | 48.778  | M146T49      |
| ESI (+)         | Imidazoleacetic acid                          | 1.620  | 0.731       | 0.023352 | 144.076 | 373.927 | M144T374     |
| ESI (+)         | Glycocholic acid                              | 1.618  | 0.454       | 0.099737 | 466.315 | 249.264 | M466T249     |
| ESI (+)         | Creatine                                      | 1.577  | 0.715       | 0.093216 | 132.076 | 339.846 | M132T340     |
| ESI (+)         | L-Carnosine                                   | 1.548  | 0.687       | 0.000152 | 227.113 | 415.126 | M227T415     |
| ESI (+)         | 3-Methylhistidine                             | 1.458  | 0.744       | 0.017674 | 170.092 | 378.842 | M170T379     |
| ESI (+)         | Stearoylcarnitine                             | 1.341  | 0.192       | 0.000025 | 428.372 | 170.293 | M428T170     |
| ESI (+)         | L-Anserine                                    | 1.311  | 0.665       | 0.000889 | 241.129 | 410.626 | M241T411     |
| ESI (+)         | Indole-2-carboxylic acid                      | 1.266  | 2.758       | 0.000636 | 162.054 | 43.026  | M162T43      |
| ESI (+)         | Methaqualone                                  | 1.221  | 0.381       | 0.002281 | 518.254 | 36.717  | M518T37      |
| ESI (+)         | Decanoyl-L-carnitine                          | 1.177  | 0.121       | 0.000008 | 316.248 | 190.189 | M316T190     |
| ESI (+)         | L-Pyroglutamic acid                           | 1.155  | 0.768       | 0.000315 | 147.076 | 368.572 | M147T369     |
| ESI (-)         | 15-keto-PGE1                                  | 5.910  | 4.875       | 0.002372 | 333.206 | 122.194 | M333T122     |
| ESI (-)         | Tricosanoic acid                              | 1.021  | 0.421       | 0.005427 | 353.341 | 39.919  | M353T40      |
| ESI (-)         | Heptadecanoic acid                            | 6.027  | 0.410       | 0.006588 | 269.249 | 41.552  | M269T42      |
| ESI (-)         | 3-Hydroxydodecanoic acid                      | 1.204  | 0.269       | 0.007140 | 237.149 | 51.664  | M237T52      |
| ESI (-)         | Indoxyl sulfate                               | 2.567  | 2.359       | 0.015048 | 212.002 | 33.597  | M212T34_1    |
| ESI (-)         | Myristic acid                                 | 2.333  | 1.227       | 0.015643 | 227.201 | 71.495  | M227T71      |
| ESI (-)         | Arachidic acid                                | 5.753  | 0.181       | 0.020543 | 311.295 | 39.513  | M311T40      |
| ESI (-)         | Deoxycholic acid                              | 1.379  | 0.173       | 0.021954 | 391.282 | 127.908 | M391T128     |
| ESI (-)         | Taurolithocholic acid                         | 1.353  | 2.008       | 0.029494 | 482.293 | 74.090  | M482T74      |
| ESI (-)         | 3,3-Dimethylglutaric acid                     | 3.492  | 0.083       | 0.029527 | 159.066 | 76.021  | M159T76      |
| ESI (-)         | Citrate                                       | 1.267  | 0.505       | 0.030858 | 191.019 | 531.020 | M191T531     |
| ESI (-)         | Azelaic acid                                  | 1.066  | 0.255       | 0.045060 | 187.097 | 340.791 | M187T341     |
| ESI (-)         | D-Ribose                                      | 2.970  | 1.611       | 0.047553 | 149.045 | 88.000  | M149T88      |
| ESI (-)         | Glycocholic acid                              | 1.292  | 0.508       | 0.048455 | 464.300 | 249.306 | M464T249     |
| ESI (-)         | DL-lactate                                    | 7.853  | 0.328       | 0.050527 | 89.025  | 225.304 | M89T225      |
| ESI (-)         | D-Fructose                                    | 1.510  | 0.510       | 0.053876 | 359.119 | 302.676 | M359T303     |
| ESI (-)         | cis-9-Palmitoleic acid                        | 7.273  | 0.264       | 0.056103 | 253.217 | 42.972  | M253T43      |
| ESI (-)         | 2-Oxadipic acid                               | 1.094  | 0.899       | 0.069544 | 181.009 | 345.477 | M181T345     |
| ESI (-)         | Stearic acid                                  | 2.292  | 0.108       | 0.070531 | 343.284 | 32.587  | M343T33      |
| ESI (-)         | Pentadecanoic Acid                            | 6.219  | 0.285       | 0.075203 | 241.217 | 44.372  | M241T44      |
| ESI (-)         | Oleic acid                                    | 16.874 | 0.395       | 0.075404 | 281.249 | 41.552  | M281T42      |
| ESI (-)         | D-Mannose                                     | 2.072  | 0.376       | 0.080779 | 239.077 | 303.095 | M239T303     |
| ESI (-)         | all cis-(6,9,12)-Linolenic acid               | 6.471  | 0.219       | 0.082966 | 277.217 | 42.262  | M277T42      |
| ESI (-)         | L-Gulonic gamma-lactone                       | 1.029  | 1.389       | 0.086900 | 237.061 | 89.228  | M237T89      |
| ESI (-)         | (+)-5,6-DHET                                  | 1.201  | 0.376       | 0.090634 | 337.237 | 125.195 | M337T125     |
| ESI (-)         | cis-Aconitate                                 | 1.636  | 1.331       | 0.091058 | 173.009 | 492.876 | M173T493     |
| ESI (-)         | Mesaconic acid                                | 1.207  | 0.430       | 0.098243 | 129.019 | 432.519 | M129T433     |

Abbreviations: m/z, mass-to-charge ratio; Rt, retention time; VIP, variance importance for projection; FC, fold change.



**Figure 5** Bioinformatics analysis of differential metabolites. a. Relevance among significant differential metabolites; b. KEGG pathway enrichment analysis of differentially expressed metabolites.

## Discussion

The yak is an ideal animal model for the study of adaptation to hypoxia at high altitudes (Ding *et al.* 2014). Metabolites in blood can be used as important reference indicators in the study of adaptation to hypoxia. The changes in measured values of relevant indicators can reflect cell activity, antioxidant capacity and the metabolic capacity of the yak, thus reflecting the adaptability of yaks to hypoxic environments (Podoinitsyna and Kozub 2019). However, the specific factors related to the metabolic cycles in the blood of yaks remain relatively unexplored. To our knowledge, this is the first study that characterized the plasma metabolomes of yaks living at different altitudes using an untargeted approach coupled with UHPLC-Q-TOF MS.

Alterations of several metabolites were observed in the blood of yaks at different altitudes of 2600 m and 4000 m on the Qinghai Plateau. In total, 52 different metabolites (ESI (+) and ESI (-) modes) associated with altitude were identified (Table 1). These metabolites were involved in the TCA cycle, histidine metabolism, fatty acid biosynthesis, glycine, serine and threonine metabolism, biosynthesis of unsaturated fatty acids and glyoxylate and dicarboxylate metabolism.

It is important to note that among all the molecules characterized, two, namely L-carnitine and Phosphatidylcholine (PC) (16:0/16:0), are recognized for their roles in metabolism. Based on the literature, the term hypoxia tends to be used to refer to the partial pressure of atmospheric oxygen, which reduces with increasing altitude. Signals from hypoxia and the resulting hypoxemia prompt the body to produce erythrocytes, which can increase the viscosity of blood and augment pulmonary arterial pressure. More recent evidence suggests that NO is a potent vasodilator and its production has been implicated in the pathogenesis of pulmonary hypertension (Ma *et al.* 2019). L-carnitine, a natural compound, exerts antioxidant effects and decreases lipid peroxidation. Carnitine can transport long-chain fatty acids, which are converted into biological energy across inner mitochondrial

membranes by alpha-oxidation (Martínez *et al.* 2004). Therefore, L-carnitine plays a critical role in oxidation to provide cellular energy. Erbas and Sharifi (Erbas *et al.* 2007; Sharifi *et al.* 2009) *et al.*, indicated that L-carnitine increased NO abundance by reducing the activity of arginase and angiotensin-converting enzyme in the aorta, heart and kidneys or by elevating NO synthase activity, resulting in higher NO production. Thus, L-carnitine can be beneficial in attenuating the oxidative stress associated with high altitudes and it demonstrates a beneficial effect in improving the cardiopulmonary function of yaks. In this study, PC (16:0/16:0) had higher VIP values, which indicated that PC (16:0/16:0) played a critical role in hypoxic adaptation and its expression level decreased with increasing altitude. PC (16:0/16:0) is a subclass of glycerophospholipids and its biological functions include membrane stability, cell signaling, fuel and energy source/storage, as well as roles in phospholipid metabolism (Chen *et al.* 2017). The higher the saturation of phospholipids, the stronger the interaction of fatty acids and the poorer the membrane fluidity, which increases the risk of atherosclerotic plaque. PC (16:0/16:0) is a saturated phospholipid and a reduction in its expression is the yak's adaptation strategy to high-altitude and low-oxygen environments. Studies suggest that PC may be recognized as a potential indicator for the prediction of the risk of vascular disease.

In general, 52 different metabolites are involved in amino acid metabolism, energy metabolism and lipid metabolism. Certain changes have occurred at different altitudes and their high VIP levels suggest the importance of these pathways in adaptation to hypoxia. It is known that mammals can utilize glycolysis, the TCA cycle and oxidative phosphorylation to generate energy from glucose. The TCA cycle is one of the hallmark pathways in energy metabolism. It is well known that this process is responsible for the oxidation of respiratory substrates to drive ATP synthesis. During hypoxia, the lack of oxygen delivery results in decreased levels of ATP, increased accumulation of lactate and alterations of

several metabolites (Cao *et al.* 2017). Jansen Seheult and colleagues have also shown that an inadequate oxygen supply slows TCA cycle-associated metabolism and leads to increased production of lactate from pyruvate (Seheult *et al.* 2017). In order to meet energy requirements under hypoxic conditions, glycolysis is enhanced, whereas the accumulation of considerable amounts of lactic acid has the potential to disrupt and damage normal physiological functions (Feenstra *et al.* 2014). This shows that in a high-altitude environment, the body generates energy by enhancing glycolysis to adapt to a low-oxygen environment. Inhibition of the TCA cycle and an increase in glycolysis metabolism under hypoxic conditions are the result of the coordinated regulation of hypoxia involving the two production pathways. In the present study, the content of lactic acid in plasma decreased with increased altitude, indicating that yaks could adapt well to high-altitude and low-oxygen environments ([http://www.kegg.jp/kegg-bin/show\\_pathway?map00020+C00158+C00417](http://www.kegg.jp/kegg-bin/show_pathway?map00020+C00158+C00417)). However, we currently have no evidence to explain the mechanisms of adaptation to lactate under hypoxic conditions.

We found that among the lipid metabolism pathways, those most affected by different altitudes involved unsaturated fatty acids and the biosynthesis of fatty acids ([http://www.kegg.jp/kegg-bin/show\\_pathway?map01040+C06425+C01530+C00712+C06426](http://www.kegg.jp/kegg-bin/show_pathway?map01040+C06425+C01530+C00712+C06426); [http://www.kegg.jp/kegg-bin/show\\_pathway?map00061+C06424+C08362+C01530+C00712](http://www.kegg.jp/kegg-bin/show_pathway?map00061+C06424+C08362+C01530+C00712)). This leads to a decrease in circulating free fatty acids, such as stearic acid, arachidic acid, oleic acid and cis-9-palmitoleic acid between the LA and HA groups, which exhibited fold changes > 2.53, indicating that lipid metabolism decreased with increasing altitude. The effect of hypoxic status on lipid metabolism is controversial and some studies suggest hypoxia as an increase or decrease in cytoplasmic lipid metabolism (Lin *et al.* 2006; Park *et al.* 2010). Additionally, another report demonstrated that the target genes of the HIF pathway that were sensitive to hypoxia could regulate lipid metabolism by activating insulin sensitivity or HIF-1 $\alpha$  could suppress fatty acid  $\beta$ -oxidation (Krishnan *et al.* 2012). It has been described that hypoxia inhibits adipogenesis by reducing PPAR $\gamma$ 2 expression (Lin *et al.* 2009; Sang *et al.* 2010). Our results are similar to those of other studies that have shown that hypoxia inhibits lipid metabolism by decreasing the expression of fatty acid metabolites, including stearic acid, arachidonic acid and oleic acid.

In amino acid metabolism, five different metabolites are enriched in histidine metabolism and glycine, serine and threonine metabolism ([http://www.kegg.jp/kegg-bin/show\\_pathway?map00340+C00386+C01262+C01152+C02835](http://www.kegg.jp/kegg-bin/show_pathway?map00340+C00386+C01262+C01152+C02835); [http://www.kegg.jp/kegg-bin/show\\_pathway?map00260+C00114+C00719+C00300](http://www.kegg.jp/kegg-bin/show_pathway?map00260+C00114+C00719+C00300)). Studies have shown that under hypoxic conditions, differentially expressed genes are significantly enriched in metabolic pathways involving glycine, serine and threonine (Xiao *et al.* 2017). Moreover, organisms can modulate the activation of oxidoreductases in glycine, serine and threonine metabolism pathways to adapt to hypoxic environments (Zhigalova *et al.* 2015).

In the present study, the lysosomal pathway exhibited the highest rich factor value, which implies that lysosomal metabolic pathways were most affected by altitude changes ([http://www.kegg.jp/kegg-bin/show\\_pathway?map04142+C00159](http://www.kegg.jp/kegg-bin/show_pathway?map04142+C00159)). We suggest that the yak relies on a lysosome-based autophagy process to remove harmful metabolites, such as excess lactic acid and fat, arising due to hypoxia to avoid cell acidosis and cardiovascular diseases such as atherosclerosis caused by fat accumulation, in order to adapt to high-altitude areas and low-oxygen environments. The lysosomal pathway is a universal catabolic process that interacts with other organelles through special membrane regions involving related organelles to achieve the transmission of metabolites and signaling molecules. Autophagy is a highly conserved process that can degrade most cytoplasmic components (Li *et al.* 2020). Additionally, autophagy is a process through which the body regulates cell metabolism and self-protection mechanisms to counter pathophysiological reactions such as injury, stress and hypoxia (Zhou *et al.* 2016). Under pathophysiological conditions, cells can remove proteins and necrotic organelles and destroy cells through autophagy, thereby maintaining homeostasis of cells and organisms (Carini *et al.* 2004; Zhou *et al.* 2016).

In conclusion, this work demonstrated the identification of metabolic pathways in the plasma of yaks associated with adaptation to hypoxia at high altitudes using UHPLC-Q-TOF/MS-based metabolomics. The results show that differences in altitude exhibit the most remarkable impact on lysosomes, energy metabolism, amino acid metabolism and fat synthesis. Yaks can better adapt to hypoxic environments by modulating metabolic pathways and interactions between various metabolic pathways.

### Acknowledgements

We are grateful to Qinwen Zhang and Haixia Jing for their assistance in sample collection.

### References

- Babar A, TD Mipam, S Wu, *et al.* 2019. Comparative iTRAQ Proteomics Identified Myocardium Proteins Associated with Hypoxia of Yak. *Current Proteomics*. 16:314-329.
- Bao P, J Pei, X Ding, *et al.* 2019. Characterisation of the complete mitochondrial genome of the Jinchuan Yak (*Bos grunniens*). *Mitochondrial DNA Part B-Resources*. 4:3856-3857.
- Cao XF, ZZ Bai, L Ma, *et al.* 2017. Metabolic Alterations of Qinghai-Tibet Plateau Pikas in Adaptation to High Altitude. *High Alt Med Biol*. 18:219-225.
- Carini R, R Castino, MG De Cesaris, *et al.* 2004. Preconditioning-induced cytoprotection in hepatocytes requires Ca<sup>2+</sup>-dependent exocytosis of lysosomes. *Journal of Cell Science*. 117:1065-1077.
- Chen Y, S Wen, M Jiang, *et al.* 2017. Atherosclerotic dyslipidemia revealed by plasma lipidomics on ApoE<sup>-/-</sup> mice fed a high-fat diet. *Atherosclerosis*. 262:78-86.
- Ding XZ, CN Liang, X Guo, *et al.* 2014. Physiological insight into the high-altitude adaptations in

- domesticated yaks (*Bos grunniens*) along the Qinghai-Tibetan Plateau altitudinal gradient. *Livestock Science.* 162:233-239.
- Erbas H, N Aydogdu, U Usta, *et al.* 2007. Protective role of carnitine in breast cancer via decreasing arginase activity and increasing nitric oxide. *Cell Biology International.* 31:1414-1419.
- Feenstra RA, MKP Kiewiet, EC Boerma, *et al.* 2014. Lactic acidosis in diabetic ketoacidosis. *BMJ Case Reports.* 2014:bcr2014203594.
- Fiehn OJPMB. 2002. Metabolomics – the link between genotypes and phenotypes. *Plant Molecular Biology.* 48:155-171.
- Gertsman I, and BA Barshop. 2018. Promises and pitfalls of untargeted metabolomics. *J Inher Metab Dis.* 41:355-366.
- Kalita HC, and R Bhattacharya. 2003. Comparative morphology of the alveolar cells in the lung of mithun (*Bos frontalis*), yak (*Bos grunniens*) and zebu (*Bos indicus*). *Indian Journal of Animal Sciences.* 73:1202-1203.
- Krishnan J, C Danzer, T Simka, *et al.* 2012. Dietary obesity-associated Hif1 $\alpha$  activation in adipocytes restricts fatty acid oxidation and energy expenditure via suppression of the Sirt2-NAD<sup>+</sup> system. *Genes Dev.* 26:259-270.
- Lan, DaoLiang, Xiong, *et al.* 2018. Transcriptome profile and unique genetic evolution of positively selected genes in yak lungs. *GENETICA – DORDRECHT.* 146:151-160.
- Li J, G Liu, L Li, *et al.* 2020. Research progress on the effect of autophagy-lysosomal pathway on tumor drug resistance. *Experimental Cell Research.* 389:111925.
- Lin Q, Z Gao, RM Alarcon, *et al.* 2009. A role of miR-27 in the regulation of adipogenesis. *FEBS J2.* 76:2348-2358.
- Lin Q, YJ Lee, and ZJJoBC Yun. 2006. Differentiation Arrest by Hypoxia. *Journal of Biological Chemistry.* 281:30678-30683.
- Ma J, L Chen, J Fan, *et al.* 2019. Dual-targeting Rutaecarpine-NO donor hybrids as novel anti-hypertensive agents by promoting release of CGRP. *European Journal of Medicinal Chemistry.* 168:146-153.
- Ma X, D Fu, M Chu, *et al.* 2020. Genome-Wide Analysis Reveals Changes in Polled Yak Long Non-coding RNAs in Skeletal Muscle Development. *Frontiers in Genetics.* 11:365.
- Martínez L, A Sánchez-Escalante, JA Beltrán, *et al.* 2004. Antioxidant effect of carnosine and carnitine in fresh beef steaks stored under modified atmosphere. *Food Chemistry.* 85:453-459.
- Nicholson JK, JC Lindon, and EJX Holmes. 1999. \ "Metabonomics\ ": understanding the metabolic responses of living systems to pathophysiological stimuli via multivariate statistical analysis of biological NMR spectroscopic data. *Xenobiotica.* 29:1181-1189.
- Park YS, Y Huang, YJ Park, *et al.* 2010. Specific down regulation of 3T3-L1 adipocyte differentiation by cell-permeable antisense HIF1 $\alpha$ -oligonucleotide. *Journal of Controlled Release.* 144:82-90.
- Podoinitsyna TA, and YA Kozub. 2019. Regular changes in hematological and biochemical indicators and immunogenetic certification of yak blood introduced in new conditions. *IOP Conference Series: Earth and Environmental Science.* 315:042007(5 pp).
- Qiu Q, G Zhang, T Ma, *et al.* 2012. The yak genome and adaptation to life at high altitude. *Nature Genetics.* 44:946-949.
- Sang YK, AY Kim, HW Lee, *et al.* 2010. miR-27a is a negative regulator of adipocyte differentiation via suppressing PPAR $\gamma$  expression. *Biochemical & Biophysical Research Communications.* 392:323-328.
- Seheult J, G Fitzpatrick, and G Boran. 2017. Lactic acidosis: an update. *Clinical Chemistry and Laboratory Medicine.* Clin Chem Lab Med. 55:322-333.
- Sharifi A, B Zare, M Keshavarz, *et al.* 2009. Effect of short term treatment of L-carnitine on tissue ACE activity in streptozotocin-induced diabetic rats. *Pathophysiology.* 16:53-56.
- Wang Q, QW Zhang, Y Zhang, *et al.* 2018. Analysis of production traits, physiological and biochemical index of yak.
- Wang Y, J Zhu, H Cai, *et al.* 2017. Crucial genes at the onset of lactation revealed by transcriptome screening of domestic yak mammary gland. *Canadian Journal of Animal Science.* 97:448-455.
- Xiao B, L Li, C Xu, *et al.* 2017. Transcriptome sequencing of the naked mole rat (*Heterocephalus glaber*) and identification of hypoxia tolerance genes. *Biology Open.* 6:1904-1912.
- Zhang X, K Wang, L Wang, *et al.* 2016. Genome-wide patterns of copy number variation in the Chinese yak genome. *Bmc Genomics.* 17:379.
- Zhigalova N, A Artemov, A Mazur, *et al.* 2015. Transcriptome sequencing revealed differences in the response of renal cancer cells to hypoxia and CoCl<sub>2</sub> treatment. *F1000Research.* 4:1518.
- Zhou J, W Shi, L-H Li, *et al.* 2016. A Lysosome-Targeting Fluorescence Off-On Probe for Imaging of Nitroreductase and Hypoxia in Live Cells. *Chemistry-an Asian Journal.* 11:2719-2724.
- Zuo H, L Han, Q Yu, *et al.* 2017. Proteomics and Bioinformatics Analyses of Differentially Expressed Proteins in Yak and Beef Cattle Muscle. *Transactions of the Chinese Society for Agricultural Machinery.* 48:313-320.